Two years of flight of the Pamela experiment: results and perspectives.

Marco Casolino[1]*, Nicola De Simone [1], Daniel Bongue[1], Maria Pia De Pascale[1], Valeria Di Felice[1], Laura Marcelli[1], Mauro Minori[1], Piergiorgio Picozza[1], Roberta Sparvoli[1], Guido Castellini[2], Oscar Adriani[3], Lorenzo Bonechi[3], Massimo Bongi[3], Sergio Bottai[3], David Fedele[3], Paolo Papini[3], Sergio Ricciarini[3], Piero Spillantini[3], Elena Taddei[3], Elena Vannuccini[3], Giancarlo Barbarino[4], Donatella Campana[4], Rita Carbone[4], Gianfranca De Rosa[4], Giuseppe Osteria[4] Mirko Boezio[5], Valter Bonvicini[5], Emiliano Mocchiutti[5], Andrea Vacchi[5], Gianluigi Zampa[5], Nicola Zampa[5], Alessandro Bruno[6], Francesco Saverio Cafagna[6], Marco Ricci[7], Petter Hofverberg[8], Mark Pearce[8], Per Carlson[8], Edward Bogomolov[9], S.Yu. Krutkov[9], N.N. Nikonov[9], G.I.Vasilyev[9], Wolfgang Menn[10], Manfred Simon[10], Arkady M. Galper[11], Lubov Grishantseva[11], Sergey Koldashov[11], Alexey Leonov[11], Vladimir V. Mikhailov[11], Sergey A. Voronov[11], Yuri T. Yurkin[11], Valeri G. Zverev[11], Galina A. Bazilevskaya[12], Alexander N. Kvashnin[12], Osman Maksumov[12], Yuri Stozhkov[12]

[1] *INFN and Physics Department of University of Rome "Tor Vergata" ,* [2] IFAC, Florence, Italy , [3] INFN and Physics Department of University of Florence , [4]INFN and Physics Department of University of Naples "Federico II" , [5]INFN, and Physics Department of University of Trieste, [6] INFN, and Physics Department of University of Bari, [7] INFN, Laboratori Nazionali di Frascati, Italy, [8]KTH, Stockholm, Sweden, [9]Ioffe Physical Technical Institute, St. Petersburg, Russia, [10] Universität Siegen, Germany , [11]Moscow Engineering and Physics Institute, Moscow, Russia, [12] Lebedev Physical Institute, Moscow, Russia

(Received October 28, 2008)

PAMELA is a satellite borne experiment designed to study with great accuracy cosmic rays of galactic, solar, and trapped nature in a wide energy range (protons: 80 MeV-700 GeV, electrons 50 MeV-400 GeV). Main objective is the study of the antimatter component: antiprotons (80 MeV-190 GeV), positrons (50 MeV-270 GeV) and search for antinuclei with a precision of the order of 10^{-8}). The experiment, housed on board the Russian Resurs-DK1 satellite, was launched on June, 15^{th} 2006 in a 350×600 km orbit with an inclination of 70 degrees. In this work we describe the scientific objectives and the performance of PAMELA in its first two years of operation. Data on protons of trapped, secondary and galactic nature - as well as measurements of the December 13^{th} 2006 Solar Particle Event - are also provided. *To appear on J. Phys. Soc. Jpn. as part of the proceedings of the International Workshop on Advances in Cosmic Ray Science March, 17-19, 2008 Waseda University, Shinjuku, Tokyo, Japan.*

KEYWORDS: cosmic rays, antimatter, dark matter, solar particle events, trapped cosmic rays

*E-mail address: casolino@roma2.infn.it

1. Introduction

The scientific program of the Wizard collaboration is devoted to the study of cosmic rays through balloon and satellite-borne devices. Aims of this research involve the precise determination of the antiproton[1] and positron[2] spectrum, search of antimatter, measurement of low energy trapped and solar cosmic rays with the NINA-1[3] and NINA-2[4] satellite experiments. Other research on board Mir and International Space Station has involved the measurement of the radiation environment, the nuclear abundances and the investigation of the Light Flash[5] phenomenon with the Sileye experiments.[6,7] PAMELA is the largest and most complex device built insofar by the collaboration, with the broadest scientific goals. In this work we describe the detector and its performance in the first two years of operations. Scientific objectives are presented together with the report of the first observations of protons of solar, trapped and galactic nature.

2. Instrument Description

The device (Figure 1) is constituted by a number of highly redundant detectors capable of identifying particles providing charge, rigidity and velocity information over a very wide energy range. A more detailed description of the device and the data handling can be found in [8–10] . The instrument is built around a permanent magnet with a silicon microstrip tracker and a scintillator system to provide trigger, charge and time of flight information. A silicon-tungsten calorimeter is used to perform hadron/lepton separation. A shower tail catcher and a neutron detector at the bottom of the apparatus are also employed to improve this separation. An anticounter system off line rejects spurious events produced in the side of the main body of the satellite. Around the detectors are housed the readout electronics, the interfaces with the CPU and all primary and secondary power supplies. All systems (power supply, readout boards etc.) are redundant with the exception of the CPU which is more tolerant to failures. The system is enclosed in a pressurized container (Figure 1) located on one side of the Resurs-DK1 satellite. In a twin pressurized container is housed the Arina experiment, devoted to the study of the low energy trapped electron and proton component. Total weight of PAMELA is 470 kg; power consumption is 355 W, geometrical factor is $21.6\,cm^2 sr$.

3. Antimatter component in cosmic rays and search for Dark Matter

The study of the antiparticle component ($\overline{p}$, e^+) of cosmic rays is the main scientific goal of PAMELA . A long term and detailed study of the antiparticle spectrum over a very wide energy range will allow to shed light over several questions of cosmic ray physics, from particle production and propagation in the galaxy to charge dependent modulation in the heliosphere to dark matter detection. See[11,12] for a discussion of the antimatter detection capabilities of PAMELA .

4. Measurement of cosmic rays in Earth's magnetosphere

Earth's magnetic field can be used as a spectrometer to separate cosmic rays of various nature and origin. To separate the primary (galactic) component from the reentrant albedo (particles produced in interactions of cosmic rays with the atmosphere below the cutoff and propagating along Earth's magnetic field line) component it is necessary to evaluate the local geomagnetic cutoff. This is estimated using the IGRF magnetic field model along the orbit; from this the McIlwain L shell is calculated.[13] In this work we have used the vertical Stormer (defined as $G = 14.9/L^2$) approximation[14] to separate between particles of different nature. Figure 2 shows the rigidity of particles as function of the evaluated cutoff G. The primary (galactic) component, with rigidities above the cutoff is clearly separated from the reentrant albedo (below cutoff) component, containing also trapped protons in the South Atlantic Anomaly (SAA).

4.1 Solar modulation of GCR

Launch of PAMELA occurred during the XXIII solar minimum. At solar minimum the magnetic field of Sun has an approximatively dipolar structure, currently with negative polarity (A<0, with magnetic field lines directed toward the sun in the northern emisphere). We are currently in an unusually long solar minimum with various predictions on the behavior of the intensity and peaking time of next maximum. In the 2006-2008 period PAMELA has been observing an increase of the flux of galactic cosmic rays at low energy (< 1 GeV) due to solar modulation caused by the decreasing solar activity. A long term measurement of the behaviour of the proton, electron and $Z \geq 2$ flux at 1 AU can provide information on propagation phenomena occurring in the heliosphere. The possibility to measure the antiparticle spectra will allow to study also charge dependent solar modulation effects.

The MDR (Maximum Detectable Rigidity) of the magnet spectrometer is $\sim 1GTV$ (700 GV on average) allows to measure the spectrum of cosmic-ray protons from 80 MeV up to almost 1 TeV; in this work we present proton data up to 200 GeV. Proton fluxes have been obtained requiring a clean track hitting the scintillator and fitted in the tracker with energy loss compatible with protons (rejecting He nuclei and secondary pions produced in the satellite). Particles of galactic origin are selected requiring that the rigidity of the event R is above the local cutoff ($R > G * 1.3$) to avoid contamination of the secondary component. To evaluate absolute spectra it was necessary to take into account live time, geometrical factor and detector efficiencies, using Montecarlo simulations (Geant 3.21) to evaluate the efficiency of each cut at various energies for each detector configuration. A compared study of the temporal and energetic variations of the efficiencies with experimental data is currently in progress. The current approach with Montecarlo simulations has an associated systematic error estimated of the order of 10% not shown in figures and tables. In Figure 4 are shown the proton fluxes measured in various periods of the mission. The effect of decreasing solar

activity on the increasing flux of cosmic rays is visible even at solar quiet period, in agreement with the increase of neutron monitor fluxes. From the flux $J(E,t)$ it is possible to evaluate the solar modulation parameter $\Phi(t)$. The heliosphere is thus approximated with a spherical structure,[15] assuming that particles lose energy independently from the sign of the charge and incoming direction to enter the heliosphere according to the following:

$$J(E,t) = \frac{E^2 - E_0^2}{(E + |Z|e\Phi(t))^2 - E_0^2} J_{is}(E + |Z|e\Phi(t)) \quad (1)$$

More detailed models involve correlation of the particle flux and solar modulation with variation with time of tilt angle of the heliospheric current sheet. In this work we have assumed a dependence of the interstellar spectrum according to:[16]

$$J_{is} = A\beta_{is}^{0.7} R_{is}^{-\gamma} \quad (2)$$

With $\beta = v/c$ and v the speed of the particle. The value of γ is obtained from the fit at high energies (from 15-20 to 200 GeV), where solar modulation effects become negligible. For PAMELA we obtain $\gamma = 2.76 \pm 0.01$. The estimation of the value of A with a precision required to estimate Φ is more complex and can affect the determination of the absolute value of Φ. In table I are shown the values of $\Phi(t)$ obtained with different assumptions of the value A. All values used are compatible with the various fits and - even though differ by as little as 2.5% - produce different values of $\Phi(t)$. It should be noted, however, that the decrease of the modulation parameter from 2006 to 2008 $\Delta\Phi_{ij} = \Phi(t_i) - \Phi(t_j)$ depends less from the assumption of A and can be considered more reliable. The values of A are shown here only to show the effect on the absolute value of solar modulation and should not be used for the evaluation of the interstellar spectrum. A more detailed estimation of A, using the full dataset of PAMELA is currently in progress.

4.2 Trapped particles in the Van Allen Belts

The high energy ($> 80MeV$) component of the proton belt, crossed in the South Pacific region can be monitored in detail with PAMELA . In Figure 3 is shown the differential energy spectrum measured in different regions of the South Atlantic Anomaly. Proton selection criteria are the same used in the determination of the absolute galactic spectrum. It is possible to see the increase of the flux toward the centre of the anomaly. Particle flux exceeds several orders of magnitude the flux of secondary (reentrant albedo) particles measured in the same cutoff region outside the anomaly and it is maximum where the magnetic field is lowest. The trapped component at the center can be fitted with energy dependent power law spectrum of the form $\phi = AE^{-\gamma-\delta E}$. This measurement can be used to validate various existing models[17,18] providing information on the trapping and interaction processes in Earth's magnetosphere. These studies will be expanded to address temporal and spatial variations as well as different particle species such as antiprotons.[19] These results can be scaled to larger but less directly accessible - magnetospheres such as Jupiter or pulsars. In Table II are shown the values obtained

fitting the trapped spectra with a rigidity dependent power law $\phi_{tr} = AR^{-\gamma-\delta R}$.

4.3 Secondary particles production in the Earth's atmosphere

In Figure 5 is shown the particle flux measured in different cutoff regions. It is possible to see the primary (galactic - above cutoff) and the secondary (reentrant albedo - below cutoff) component. At the poles, where field lines are open and cutoff is below the minimum detection threshold of PAMELA the secondary component is not present. Moving toward lower latitude regions the cutoff increases and it is possible to see the two components, with the position of the gap increasing with the increase of the cutoff. The secondary component of cosmic rays contributes to the atmospheric neutrino production.[20] Therefore an accurate measurement of the secondary component is of relevance in the reduction of the uncertainties of the expected flux on the ground[21] and in the estimation of hadronic cross sections (protons on O or N) at high energies, not otherwise determinable on ground.

5. Solar energetic particles

PAMELA observations are currently taking place at the solar minimum of XXIII cycle. Currently only one series of major solar events in December 2006 has been detected. It is expected that in the next years, going toward XXIV cycle solar maximum, more events will be detected by the apparatus. The characteristics of PAMELA allow real time measurements of different particle spectra, important in understanding the acceleration and propagation mechanisms which take place at the Sun and in the heliosphere. In this section we briefly discuss the observation capabilities of PAMELA and report on the proton spectra observed in the December event.

5.1 Electrons and positrons

Positrons are produced mainly in the decay of π^+ coming from nuclear reactions occurring at the flare site. Up to now, they have only been measured indirectly by remote sensing of the gamma ray annihilation line at 511 keV. Using the magnetic spectrometer of PAMELA it will be possible to separately analyze the high energy tail of the electron and positron spectra at 1 Astronomical Unit (AU) obtaining information both on particle production and charge dependent propagation in the heliosphere in perturbed conditions of Solar Particle Events.

5.2 Protons and nuclei

PAMELA can measure the solar component over a very wide energy range (where the upper limit will be determined by the size and the spectral shape of the event). These measurements can be correlated with other instruments placed in different points of the Earth's magnetosphere to give information on the acceleration and propagation mechanisms of SEP (Solar Energetic Particle) events. Up to PAMELA measurements there has been no direct measurement[22] of the high energy (>1 GeV) proton component of SEPs. Until now the spectrum of solar energetic particles covering the energy range from $\simeq$ MeV/n to at least several GeV/n could not be measured by a single device; spacecraft, balloon, and neutron monitor

data currently being used for this purpose.[41] Moreover, the energy range of onboard spectrometers have some problems with > 100 MeV energy channels due to particles penetrating the detector from the side.[42] Since the majority of solar energetic particle events have a spectrum turnover around 100 MeV/n[23] it is extremely important to measure the whole energy range of solar energetic particles by a single instrument. Another important task is to find the upper limit of acceleration processes at the Sun. Also the light nuclear component related to SEP events over a wide energy range can be investigated. This should contribute to establish whether there are differences between the compositions of the high energy (1 GeV) and the low energy component ($\simeq$ 20 MeV) ions producing γ rays or the quiescent solar corona.[25] These measurements will help us to better understand the selective acceleration processes in the higher energy impulsive events.[26]

5.3 13 December 2006 Solar Particle Event

At the time of writing the most significant events detected by PAMELA occurred between December 6^{th} and 17^{th} 2006 and were originated from active region NOAA 10930. Dec 6^{th} event was originated in the East limb, resulting in a gradual proton event reaching Earth on Dec 7^{th} and lasting until the events of Dec 13 and 14.[27] On 13^{th} December 2006, 02:38 UT an X3.4/4B solar flare occurred in active region NOAA 10930 ($S06^{o}W23^{o}$). The interaction between the fast rotating sunspot and the ephemeral regions triggers continual brightening and finally produces the major flare.[28] The intensity of the event is quite unusual for a solar minimum condition. Starting at 2:50 UT on the same day various neutron monitors, with cutoff rigidities below about $4.5\,GV$, recorded a Ground Level Enhancement (GLE70) with relative increases ranging from 20% up to more than 80% (Apaty, Oulu).[29,30] Apaty and Oulu also registered the peak of the event beetween 02:40 UT and 03:10 UT, while most of the neutron monitors had it between 03:10 UT and 03:40 UT. The spectrum and its dynamic was investigated at higher energies using ground measurements by neutron monitors at different cutoff rigidities[31] resulting in a spectral estimation assuming a power law in rigidity of $\gamma \simeq 6$. The onset time was later for the proton channels on-board of GOES-11 satellite: 03:00 UT for greater than 100 MeV protons and 03:10 for greater than 10 MeV protons.[30] PAMELA was in an high cutoff region at the flare occurrence and reached the South Polar region at about 03:10 UT. Muon monitors were also able to detect the GLE event and its spatial-angular anisotropy has been measured.[32] Differential proton spectra were directly meausured by GOES, ACE, Stereo, SAMPEX at energies below $400\,MeV$. With these instruments it was also possibile to measure the elemental composition of the various events.[33,34]

The event produced also a full-halo Coronal Mass Ejection (CME) with a projected speed in the sky of 1774 km/s.[35] The forward shock of the CME reached Earth at 14:38 UT on December 14, causing a Forbush decrease of galactic cosmic rays which lasted for several days.

In Figure 6 is shown the differential energy spectrum measured with PAMELA in different periods of the event. It is possible to see that particles were accelerated up to 3-4 GeV.

A second smaller event occurred in conjunction with a X1.5 flare from the same active region (NOAA 10930, $S06^oW46^o$) on Dec 14, superimposing on the Forbush decrease caused by the Coronal Mass Ejection of the previous event reaching Earth. Galactic particle flux thus decreased in the energy range up to 3 GeV, whereas solar particles were accelerated up to 1 GeV for this event. The decrease was also observed by Wind, Stereo and Polar but not by the GOES satellites, with the exception of some variation in the 15-40 MeV channel of GOES-12.[36] In case of PAMELA the relative decrease record by was up to more than 20%, extending above 5 GeV.

The good energetic resolution and the statistic of the event allows for a detailed study of the temporal variations of the spectrum of this event in the energy range 100 MeV - 5 GeV, an interval usually not studied in detail with spaceborne detectors and usually accessible through ground neutron monitors. In Figure 7 is shown the rigidity spectrum at the beginning of the event (3:18 - 3:23 GMT 13/12/2006, after subtraction of the galactic component) fitted with various functions (exponential in kinetic energy E, rigidity R, rigidity dependent power law, Bessel function):

$$\phi = A\, e^{-\frac{E}{E_0}} \tag{3}$$

$$\phi = A\, e^{-\frac{R}{R_0}} \tag{4}$$

$$\phi = A\, R^{-\gamma-\delta(R-1)} \tag{5}$$

$$\phi = A\, p\, K_2\left(2\sqrt{3\frac{p}{c\alpha T}}\right) \tag{6}$$

The various functions are representative of acceleration and propagation processes under different hypothesis.[37] K_2 is a modified Bessel function of order 2, with αT as free parameter - α representing an acceleration rate and T the escape time from the acceleration region, with their product higher in larger events. This function is a solution of a stochastic Fermi acceleration[38–40] in the non-relativistic limit and therefore is best suited for energies below $\simeq GeV$. From the Figure it is possible to see that all fits are qualitatively good, given the small number of free parameters, the large energy range of the fit and the experimental uncertainties. χ^2 values are high (75, 148, 86, 420 respectively according to the list of formulae above). The best fit is obtained for the exponential in energy ($E_0 = 380MeV$) which approximates better the shape of the function in the intermediate energy range. The exponential in rigidity ($R_0 = 290$ MV) is however better in reproducing the observed spectrum at high energies. To study the evolution of the particle spectrum of the event we have fitted the spectra at various times with Bessel functions (see Figure 8) plotting the results of the fit in Figure 9, top panel. With the passage of time the intensity of the spectrum increases (due to the increasing flux at

low energy) with the lowering of αT implying a decrease of the acceleration phenomenon. It is interesting to note that the values obtained are compatible to what found for other events at lower energies in the energy range 10-100 MeV,[37] sign that a similar description of the acceleration and propagation phenomena is valid at higher energies. Note however that at this stage we do not infer any conclusion on these processes from the spectral shape of fit performed. The same spectra have also been fitted with a rigidity dependent power law. This spectral shape better describes the decrease of the flux in the lowering of the value of A with time, shown in Figure 9, bottom panel. It is also possible to observe high value of δ at the beginning of the event, implying deviation from a shock accelerated spectrum. The values of δ decrease and get close to zero after some hours showing how the spectrum becomes more similar to a single power law and therefore possibly better representative of a shock accelerated structure. Further studies will involve other particle species (He, e^-) and long term effects such as the Forbush decrease.

6. Conclusions

PAMELA was successfully launched on June 2006. Is currently operational in Low Earth Orbit and has recently passed two years of operation. We have presented some measurements of protons of galactic, solar and trapped/secondary origin showing that the satellite and the detectors are functioning correctly and providing new data on the particle and antiparticle component of cosmic rays.

References

1) M. Boezio, et al., ApJ 487 (1997) 415.
2) M. Boezio, et al., ApJ 532 (2000) 653–669.
3) V. Bidoli, et al., ApJS 132 (2001) 365–375.
4) V. Bidoli, et al., Journal of Geophysical Research (Space Physics) 108 (2003) 1211.
5) M. Casolino, et al., Nature 422 (2003) 680.
6) V. Bidoli, et al., Journal of Physics G Nuclear Physics 27 (2001) 2051–2064.
7) M. Casolino, et al., Advances in Space Research 37 (2006) 1691–1696.
8) P. Picozza, et al., Astroparticle Physics 27 (2007) 296–315.
9) M. Casolino, et al., Advances in Space Research 37 (2006) 1857–1861.
10) M. Casolino, et al., Advances in Space Research 37 (2006) 1884–1888.
11) M. Casolino, P. Picozza, Advances in Space Research 41 (2008) 2064–2070.
12) M. Casolino, P. Picozza et al., Advances in Space Research 42 (2008) 455–466, arXiv:0708.1808.
13) Tech. rep., IAGA (2005).
14) M. A. Shea, et al., Physics of the Earth and Planetary Interiors 48 (1987) 200–205.
15) L. J. Gleeson, W. I. Axford, Solar Modulation of Galactic Cosmic Rays, ApJ154 (1968) 1011.
16) Y. Shikaze, S. Haino, et al., , Astroparticle Physics 28 (2007) 154–167.
17) J. D. Gaffey, Jr., et al., Journal of Spacecraft and Rockets 31 (1994) 172–176.
18) R. S. Selesnick, et al., Space Weather 5 (2007) S04003.
19) R. S. Selesnick, et al., Geophysical Research Letters34 (2007) 20104.
20) M. Honda, et al., Physical Review D70 (4) (2004) 043008.
21) T. Sanuki, et al., Physical Review D75 (4) (2007) 043005.
22) L. I. Miroshnichenko (Ed.), Vol. 260 of Astrophysics and Space Science Library, 2001.
23) J. M. Ryan, Space Science Reviews 93 (2000) 581–610.
24) G. A. Bazilevskaya, et al., Space Science Reviews 85 (1998) 431–521.
25) J. M. Ryan, in: International Cosmic Ray Conference, Vol. 10 of International Cosmic Ray Conference, 2005, pp. 357.
26) D. V. Reames, Space Science Reviews 90 (1999) 413–491.
27) D. Wilkinson, Tech. rep., NOAA's National Geophysical Data Center (2006).
28) J. Zhang, et al., ApJl 662 (2007) L35–L38.
29) J. W. Bieber, et al., in: ICRC 2007 Proceedings.
30) Y. Q. Tang, in: ICRC 2007 Proceedings.
31) E. Vashenyuk, et al., in: ICRC 2007 Proceedings.
32) D. A. Timashkov, et al., in: ICRC 2007 Proceedings.
33) R. A. Mewaldt, et al., in: ICRC 2007 Proceedings.
34) C. M. S. Cohen, et al., in: ICRC 2007 Proceedings.
35) Y. Liu, et al., ArXiv e-prints 802.
36) T. Mulligan, et al., in: ICRC 2007 Proceedings.
37) R. E. McGuire, T. T. von Rosenvinge, F. B. MacDonald, in: International Cosmic Ray Conference, Vol. 3 of International Cosmic Ray Conference, 1981, pp. 65–68.
38) R. Ramaty, in: J. Arons, C. McKee, C. Max (Eds.), Particle Acceleration Mechanisms in Astrophysics, Vol. 56 of American Institute of Physics Conference Series, 1979, pp. 135–154.

Table I. Solar modulation parameter obtained with the fit of the proton spectrum in different periods. Note the dependence of Φ from the assumed value of the absolute spectrum A . The variations of Φ are however more independent from A.

A p/(cm^2 s sr GeV^{-1} GV$^{-2.76}$)	2.0	1.95	1.91
	Φ (MV)		
July 2006	635 ± 3	627 ± 2	621 ± 3
August 2007	565 ± 2	558 ± 3	552 ± 3
February 2008	561 ± 3	553 ± 2	546 ± 2

Table II. Fit of the core regions of the SAA according to a rigidity dependent power law spectrum.

Region G	A $p/cm^2s\,srGeV$	γ	δ GV^{-1}	χ^2 /ndf
$0.19 < B$	4.0 ± 0.4	3.6 ± 0.6	2.0 ± 0.4	0.04
$0.19 < B < 0.20$	1.0 ± 0.1	4.6 ± 0.8	1.6 ± 0.5	0.17
$0.20 < B < 0.21$	0.05 ± 0.008	5.6 ± 1.5	0.8 ± 1.4	0.40

39) J. A. Miller, N. Guessoum, R. Ramaty, ApJ361 (1990) 701–708.

40) W. Q. Gan, ApJ496 (1998) 992.

41) Bazilevskaya G.A., Solar cosmic rays in the near Earth space and the atmosphere, Adv. Space Res., 2005, v. 35, No. 3, p. 458-464

42) Smart D.F., Shea M.A. Comment on the use of GOES solar proton data and spectra in solar dose calculations. Radiation Measurements, 1999. 30(3). p. 327-335.

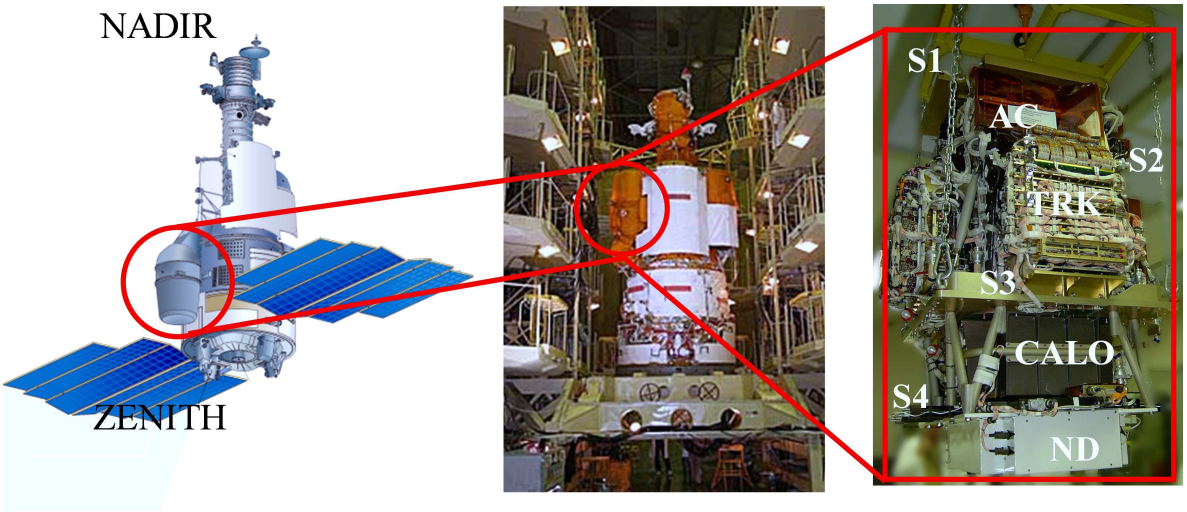

Fig. 1. Left: Scheme of the Resurs-DK1 satellite. PAMELA is located in the pressurized container on the left of the picture. In the scheme the pressurized container is in the acquisition configuration. Center: The Resurs-DK1 satellite during integration in Samara. The pressurized container housing Pamela is in the folded (launch) position. Right: Photo of the PAMELA detector in Tor Vergata with marked the position of the detectors. S1, S2, S3, S4: scintillator planes; AC: top anticoincidence; TRK: tracker core; CALO: Silicon-Tungsten calorimeter; ND: Neutron Detector.

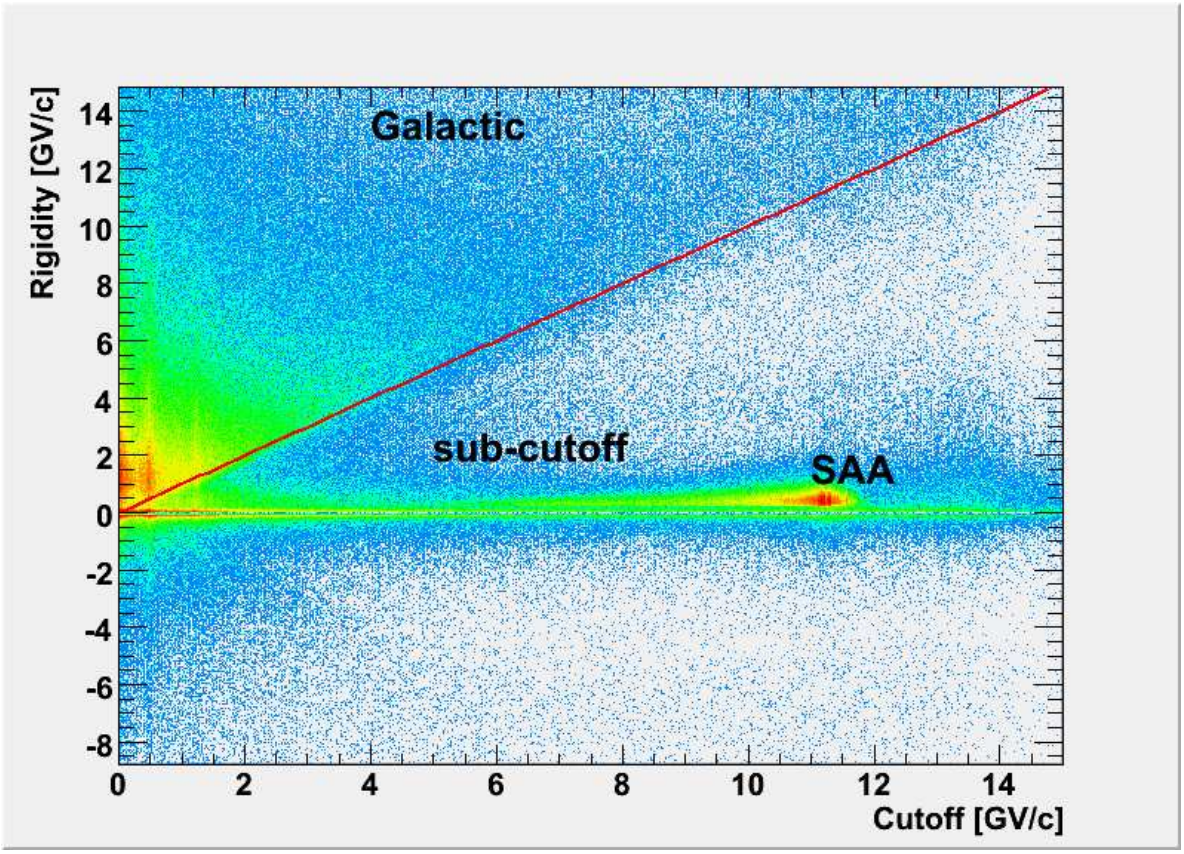

Fig. 2. Histogram of the rigidity R_{tr} measured in the tracker vs vertical Stormer Cutoff. Particles with positive charge (p, e^+) have $R_{tr} > 0$ and particles with negative charge have $R_{tr} < 0$. The effect of the geomagnetic field on galactic particles is clearly visible. Primary particles, of galactic or solar origin, have a rigidity above the local Stormer cutoff (see text) and are well separated from reentrant albedo events (below the cutoff) produced in the interaction of primaries with the Earth's atmosphere. It is also possible to see the spot of high fluence of low ($R < 2$ GV) protons trapped in the inner Van Allen belt, crossed by PAMELA in the South Atlantic Anomaly (SAA) region.

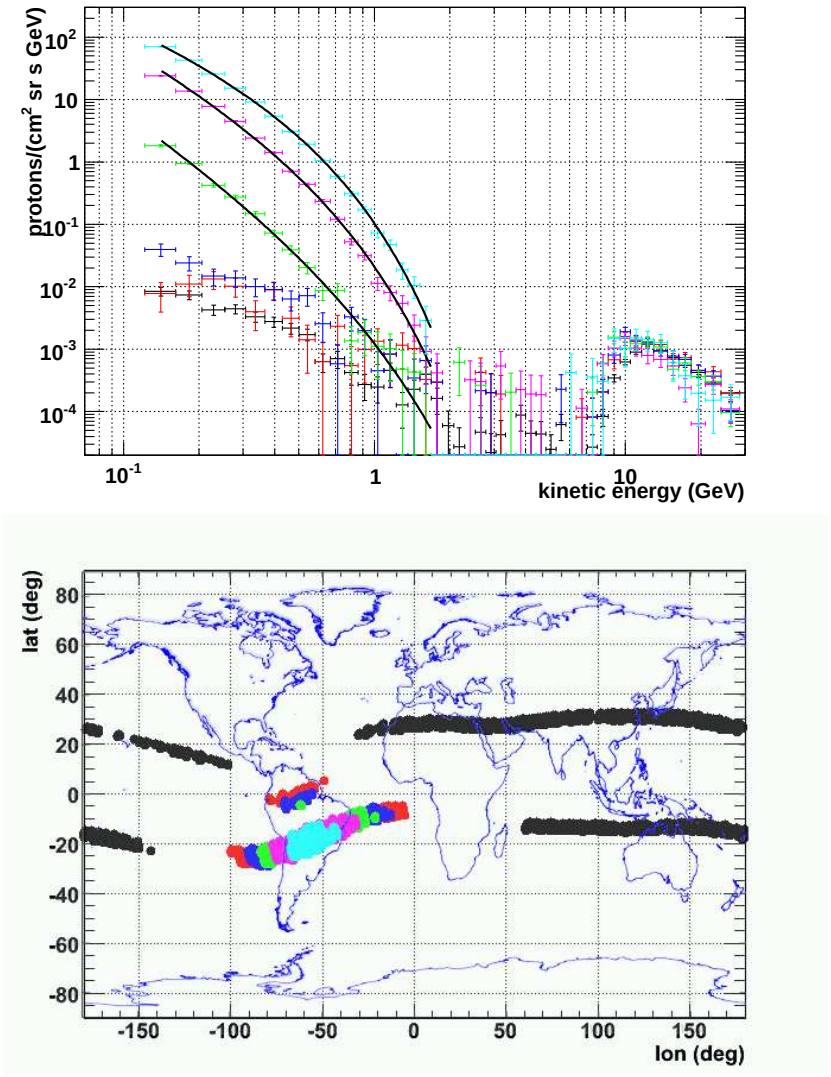

Fig. 3. Top: Plot of the differential energy spectrum of PAMELA in different regions of the South Atlantic Anomaly. Selection regions (shown in top bottom panel) are selected according to decreasing intensity of the magnetic field from bottom to top: Black $B > 0.3G$ - outside the SAA, Red 0.22 G $< B <$ 0.23 G, Blue 0.21 G $< B <$ 0.22 G, Green $0.20G$ ¡ B ¡ 0.21 $G, Pink$ 0.19 G $< B <$ 0.20 G, Turquoise 0.19 G ¿ B) in the cutoff region 10.8 GV $< G <$ 11.5 GV. Flux of trapped particles can exceed the secondary particle flux in the same cutoff region outside the anomaly (black bands) of about four orders of magnitude at low energy.

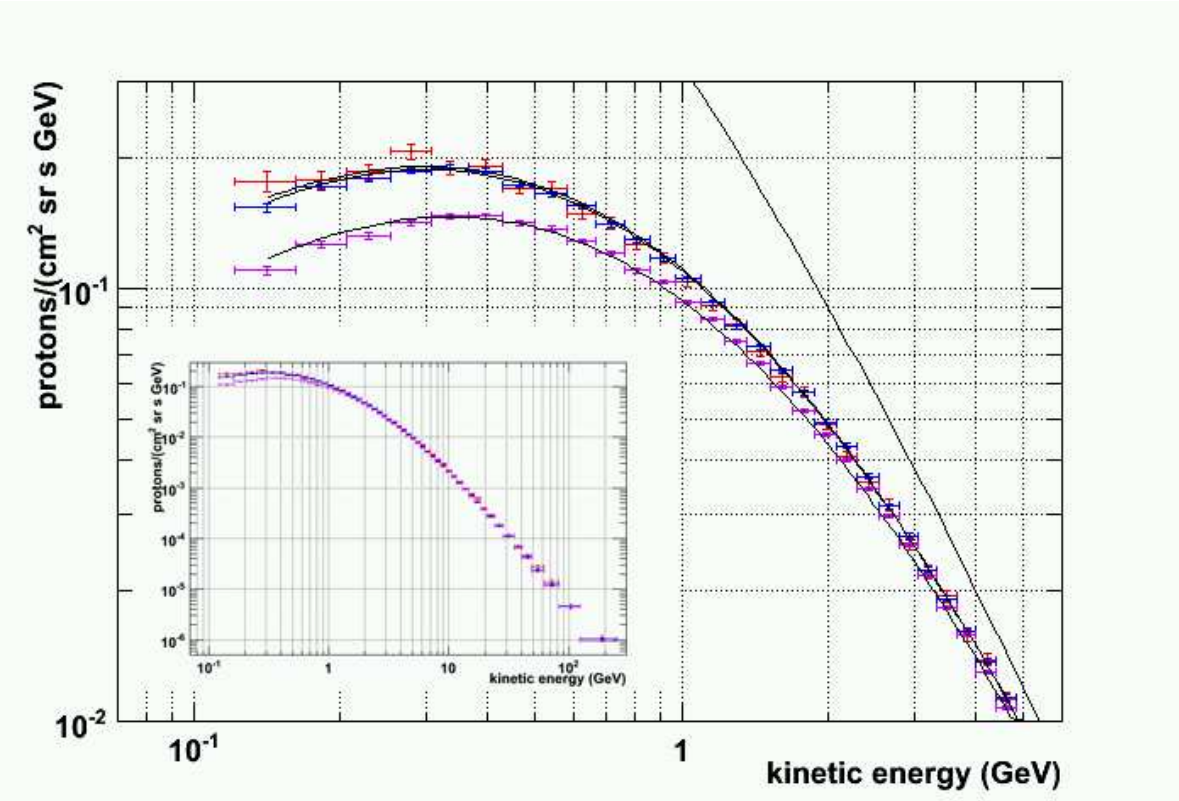

Fig. 4. Differential spectrum of protons measured in July 2006 (purple - bottom), August 2007 (black - central), February 2008 (red - top curve). Below 1 GeV it is possible to see the effect of solar modulation on the flux variation. The straight black line represent the assumed interstellar spectrum. Only statistical errors are shown.

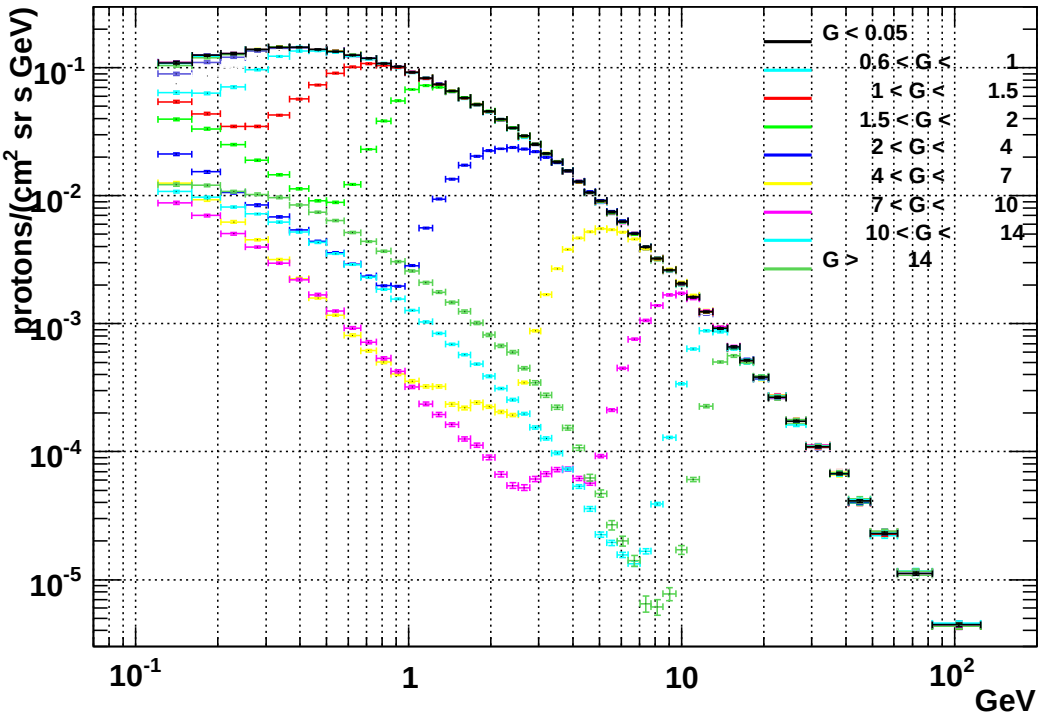

Fig. 5. Plot of the differential energy spectrum of PAMELA at different values of geomagnetic cutoff G. It is possible to see the primary spectrum at high rigidities and the reentrant albedo (secondary) flux at low rigidities. Only statistical errors are shown.

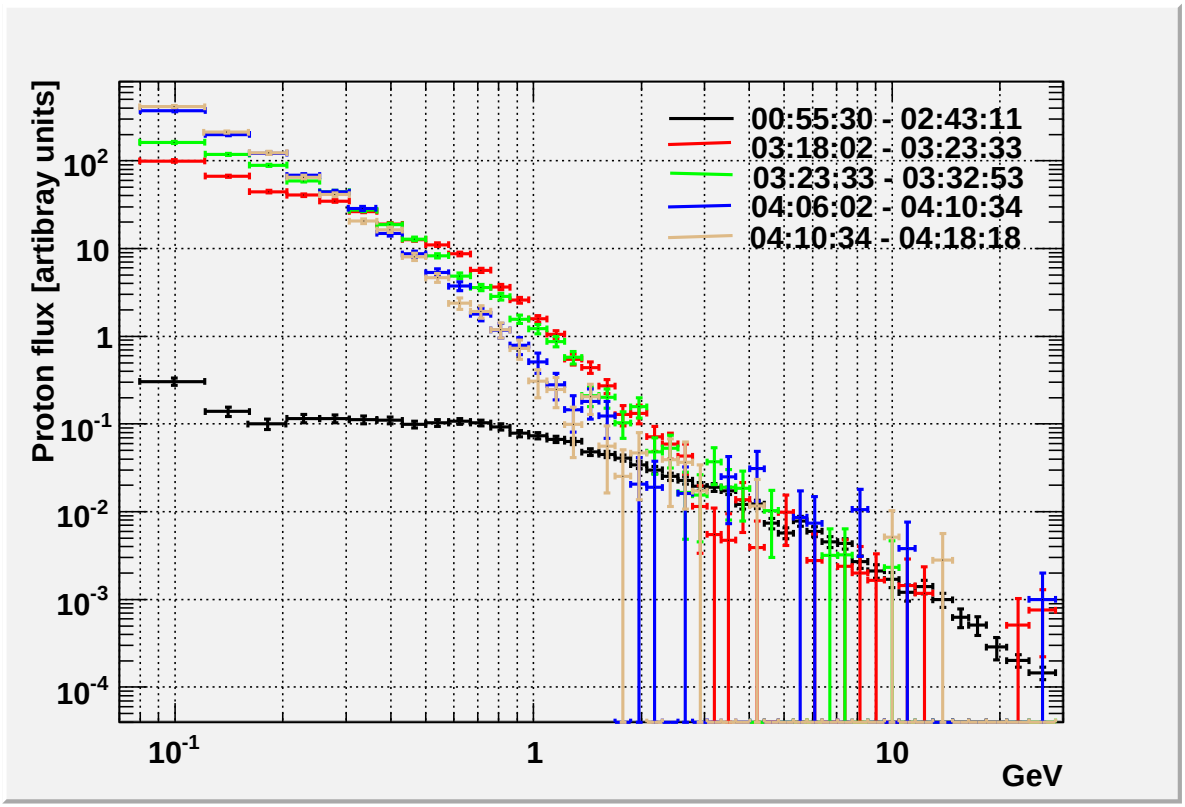

Fig. 6. Proton differential energy spectra (flux vs kinetic energy) in different time intervals during the event of the 13th December 2006. The black line is the spectrum before the arrival of the charged particles with a small peak at low energy due to the presence of solar protons from previous events. It can be observed that the maximum flux of the high energy component of the solar protons arrives at the beginning of the event while only one hour later the maximum flux at low energy is detected. On the other hand, the flux at high energy decreases faster than at low energy. Only statistical errors are shown.

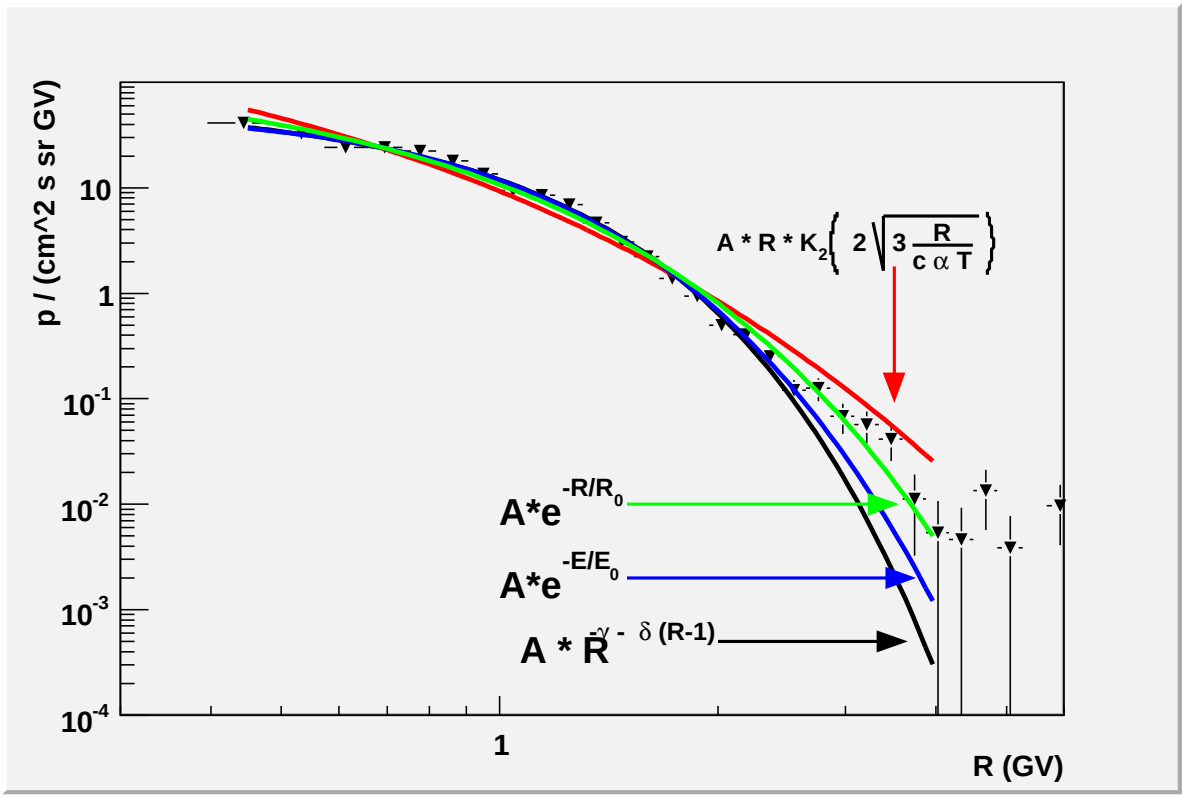

Fig. 7. Fit of the proton rigidity spectra at the beginning of the event. Different functions have been employed: from top to bottom at the high end of rigidity (red: Bessel K2 function, green Exponential in rigidity, blue: Exponential in energy, Black exponential in rigidity. Best fit function according to χ^2 is the exponential in kinetic energy.)

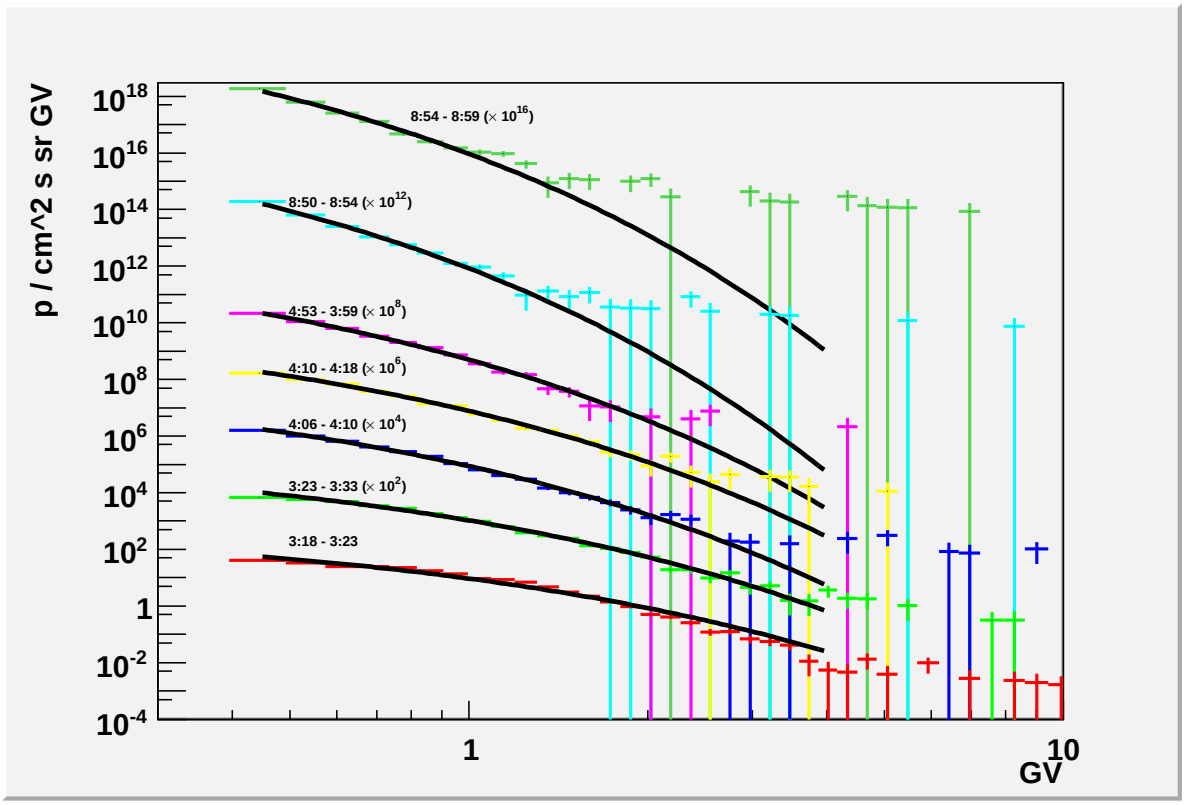

Fig. 8. Proton differential energy spectra with galactic flux subtracted in different time intervals during the event of the 13th December 2006. The fluxes have been scaled in the plot. The fit with Bessel K2 function. Only statistical errors are shown.

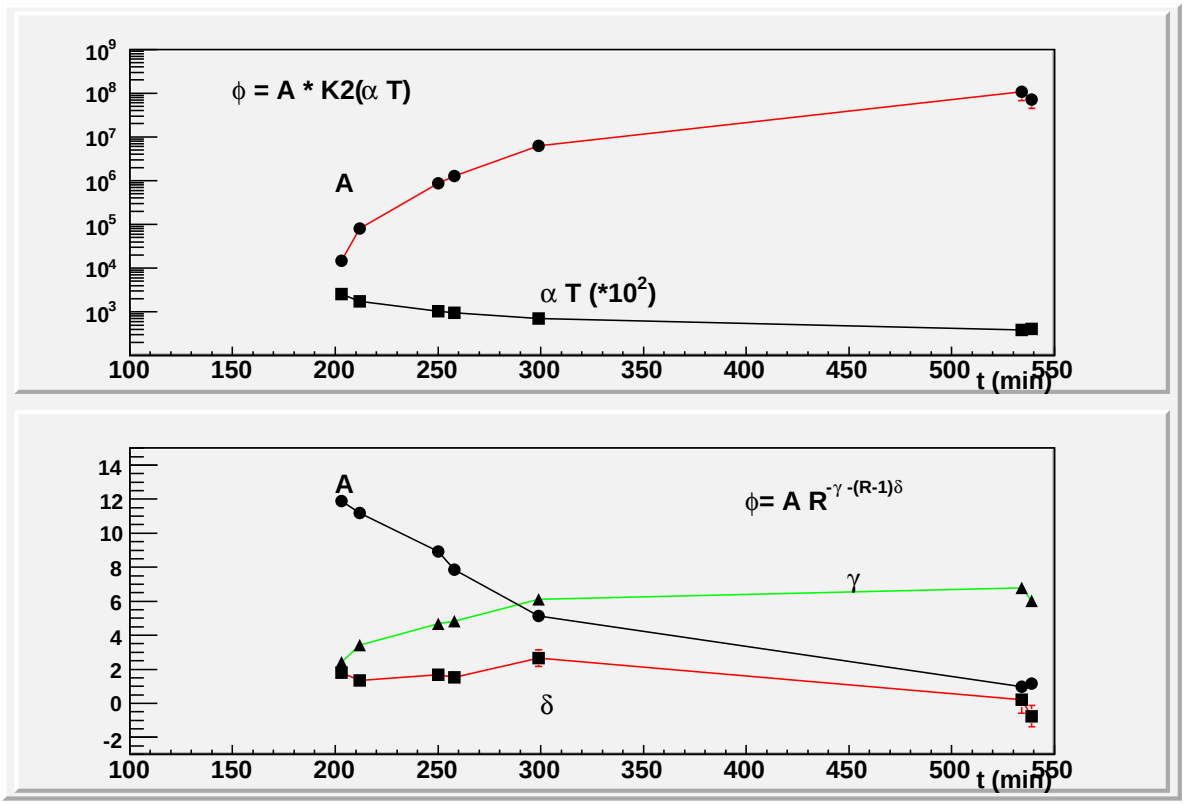

Fig. 9. Top Panel: Fit of the Rigidity proton spectra with Bessel K2 function as function of time (minutes from 2006-12-13-00:00 GMT) . Top line: Absolute value. Bottom line: αT. It is possible to see how particle flux increases and αT decreases with time. Bottom Panel: Fit of the Proton spectra with Rigidity dependent power law as function of time ($\phi = AR^{-(\gamma+\delta(R-1))}$) (from top to bottom: A, γ, δ). In this case particle flux decreases with time. The decrease of the rigidity dependent term δ implies a straightening of the spectrum.